J Wood Sci (2011) 57:71–75
DOI 10.1007/s10086-010-1140-3

NOTE

Mako Yamamoto · Tsuguyuki Saito · Akira Isogai
Manabu Kurita · Teiji Kondo · Toru Taniguchi
Rumi Kaida · Keiichi Baba · Takahisa Hayashi

Enlargement of individual cellulose microfibrils in transgenic poplars overexpressing xyloglucanase

Received: May 10, 2010 / Accepted: June 15, 2010 / Published online: October 7, 2010

Abstract Holocellulose samples prepared from transgenic poplars overexpressing xyloglucanase had crystal widths of 3.2–3.5 nm as a result of the (2 0 0) plane, based on their X-ray diffraction patterns, and crystal widths were greater than those of the wild type (3.0 nm). Cellulose microfibril widths in the holocellulose samples were further determined from transmission electron microscopic (TEM) images of individualized fibrils prepared by 2,2,6,6-tetramethylpiperidine-1-oxy radical-mediated oxidation of the holocelluloses and the successive disintegration of the oxidized products in water. The TEM images also supported the finding that cellulose microfibril widths of transgenic poplars were larger than those of the wild type. The cellulose microfibril widths of transgenic poplars were approximately 6 nm, whereas those of the wild type were about 5 nm. However, such enlargement of cellulose microfibril widths could not be explained by the increased cellulose contents of the transgenic poplars alone.

Key words Transgenic poplar · Xyloglucanase · Cellulose fibril · TEMPO-mediated oxidation

Introduction

Two lines (trg300-1 and trg300-2) of transgenic poplars were selected from 54 independent transgenic lines that expressed *Aspergillus aculeatus* xyloglucanase (AaXEG2) under the control of a constitutive promoter.[1] These lines are currently being used in an open field plantation as part of a field trial of transgenic plants in Japan lasting from March 2007 to December 2010.[2]

Xyloglucan serves as a key hemicellulose for tightening tethers between cellulose microfibrils in the secondary wall and in the primary wall. There is evidence that xyloglucan tightens gelatinous layers to the S2 layer in the secondary walls and provides tension in the wall structure.[3,4] It has been shown that if the tether is loosened during growth, trees placed horizontally are unable to bend upward.[1,5–7] The cellulose microfibrils of this wood could also be easily hydrolyzed by fungal cellulase.[8] We have concluded that the genetic reduction of xyloglucan in xylem could transform the bundles of cellulose microfibrils in wood. Such technology could be used in either fibril or wall modification.

Wood cellulose microfibril widths have been studied primarily from transmission electron microscopic (TEM) images of fibrillated celluloses, and were reported to be in the range 1.5–5 nm.[9–11] Recently, the separation of individual microfibrils has been achieved by catalytic oxidation of the fibril surfaces using the 2,2,6,6-tetramethylpiperidine-1-oxyl radical (TEMPO).[12,13] TEMPO-mediated oxidation can selectively oxidize the C6 hydroxyl groups on the microfibril surfaces to carboxyls, which have anionic charges in water.[14] A repulsive effect works between the fibrils, and, consequently, the oxidized celluloses disperse in water as individual microfibrils, assisted by mild mechanical disintegration. This method seems to be effective in evaluating the size of cellulose microfibrils by transmission electron or atomic force microscopy, since the microfibrils become well separated in water without any decrease in the original microfibril width.[12–14]

In the present study, we evaluated the sizes of cellulose microfibrils in open-field-grown transgenic poplars in terms of crystal width calculated from the X-ray diffraction patterns of cellulose and microfibril width obtained from the microscope images of the microfibrils separated by the TEMPO-oxidation method.

M. Yamamoto · T. Saito · A. Isogai (✉)
Graduate School of Agricultural and Life Sciences, The University of Tokyo, 1-1-1 Yayoi, Bunkyo-ku, Tokyo 113-8657, Japan
Tel. +81-3-5841-5538; Fax +81+3-5841-5269
e-mail: aisogai@mail.ecc.u-tokyo.ac.jp

M. Kurita
Forest Bio-Research Center, Forestry and Forest Products Research Institute, Hitachi, Ibaraki 319-1301, Japan

T. Kondo · T. Taniguchi
Forest Tree Breeding Center, Forestry and Forest Products Research Institute, Hitachi, Ibaraki 319-1301, Japan

R. Kaida · K. Baba · T. Hayashi
RISH & Institute of Sustainability Science, Kyoto University, Uji 611-0011, Japan

Experimental

Materials

Transgenic poplars overexpressing xyloglucanase (AaXEG, AY160774) were produced with the signal peptide of PaPopCel1 under control of the CaMV35S promoter, as reported previously.[1] The signal peptide of PaPopCel1 (D32166) was used for secretion.[5] The poplars used in this study were from the trg300-1 and trg300-2 lines and had been grown in an open field for 2 years.[2]

The bark and cambium layer were stripped and removed from the stem. The remaining xylem was cut into small pieces by scissors and soaked in 90% (v/v) aqueous acetone for 1 day in order to remove extractives. The defatted wood pieces (2.5 g) were then bleached with $NaClO_2$ (1 g) in 0.13% acetic acid (150 ml) for 1 h at 70°–80°C.[15] This procedure was repeated four times to prepare holocellulose samples, which were then disintegrated in water using a mechanical homogenizer (Physcotron, Microtec, Japan). The obtained holocellulose fibers were collected by filtration and stored at 4°C before use. The holocellulose was extracted four times with 24% KOH containing 0.1% $NaBH_4$ and separated into alkali-soluble and -insoluble fractions.

The total sugar in each fraction was determined by the phenol–sulfuric acid method.[16] The alkali-soluble fraction was neutralized, dialyzed, and subjected to acid hydrolysis.[17] Alditol acetates of the hydrolysates were analyzed using an Agilent gas chromatograph with a DB-225 glass capillary column (15 m).

TEMPO-mediated oxidation

The holocellulose sample (1 g) was suspended in water (100 ml) containing TEMPO (0.016 g, 0.1 mmol) and sodium bromide (0.1 g, 1 mmol). TEMPO-mediated oxidation was initiated by adding a predetermined amount of the 12% NaClO solution (5.0 mmol NaClO per gram of cellulose) and continued at room temperature by stirring at 500 rpm. The pH was maintained at 10 by adding 0.5 M NaOH using a pH stat until no NaOH consumption was observed.[14,18] The TEMPO-oxidized holocellulose was thoroughly washed with water by filtration and stored at 4°C before further treatment or analysis.

Mechanical fibrillation of TEMPO-oxidized holocellulose

The wet TEMPO-oxidized holocellulose was suspended in water (20 ml) at a consistency of 0.1% (w/v) and a pH of 7–8. The suspension was sonicated for 2 min using an ultrasonic homogenizer (US-300T, Nihonseiki, Japan) at 19.5 kHz and an output power of 300 W (7 mm probe tip diameter).[12,13] The suspension was then centrifuged at 10 000 *g* to separate a transparent and viscous supernatant from the unfibrillated and partially fibrillated fractions. More than 80% of the TEMPO-oxidized holocellulose was dispersed in the supernatant fraction by this treatment.

Analyses

The holocellulose samples were observed with an optical microscope (Olympus BX50). X-ray diffraction patterns were recorded for freeze-dried and then pressed samples using the reflection method by means of a Rigaku RINT 2000 with monochromator-treated Cu K_α radiation (λ = 0.15418 nm) at 40 kV and 40 mA. Crystal widths were calculated from the full width of half-height diffraction due to the (2 0 0) plane using Scherrer's equation[19] after dividing the peak from the background using pseudo-Voigt and cubic functions, respectively. The crystallinity index of cellulose I was determined from the ratio of the separated peak area due to cellulose I to the total area from 5° to 30° of 2θ.[20] The cellulose microfibrils separated in water by the TEMPO-oxidation method were observed after drying on a glow-discharged carbon-coated Cu grid with a JEOL JEM-2000EX microscope operated at an accelerating voltage of 100 kV. The TEM images were taken under diffraction contrast in bright-field mode using a low dose exposure.[21] The average microfibril or fiber width and its standard deviation were obtained by measuring 20 microfibrils in TEM images or 9–14 fibers in optical microscopic images for each sample. Statistically significant differences in the width between two samples were evaluated using the unpaired *t* test in both homo- and heteroscedastic cases.

Results and discussion

Fiber width and morphology

Figure 1 shows optical microscopic images of fibers of the holocellulose samples prepared from wild-type and transgenic poplars. The fiber morphologies were visually similar. Moreover, the average widths of the fibers were 17.8 ± 2.3, 18.5 ± 2.1, and 17.5 ± 2.0 μm for the wild-type, trg300-1, and trg300-2 poplars, respectively. Because all *P* values calculated for statistical estimation of any two-sample combinations were greater than 0.2, it can be concluded that the three samples had similar fiber widths and no statistically significant difference in fiber width was observed among the three samples. Thus, prevention of xyloglucan deposition in the fibers of transgenic poplars is likely to have almost no influence on the wood fiber width.

X-ray diffraction patterns

The X-ray diffraction patterns of holocelluloses prepared from the transgenic and wild-type poplar samples showed the typical cellulose I allomorph (Fig. 2). Because hemicelluloses were present in the holocelluloses, their crystallinity indices were relatively low, and ranged from 0.31 to 0.33 (Table 1). The crystallinity indices of the transgenic poplar samples were slightly higher than that of the wild type. The crystal widths calculated from the full width of half-height diffraction due to the (2 0 0) plane were more clearly different between the three samples: 0.30, 0.32, and 0.35 nm

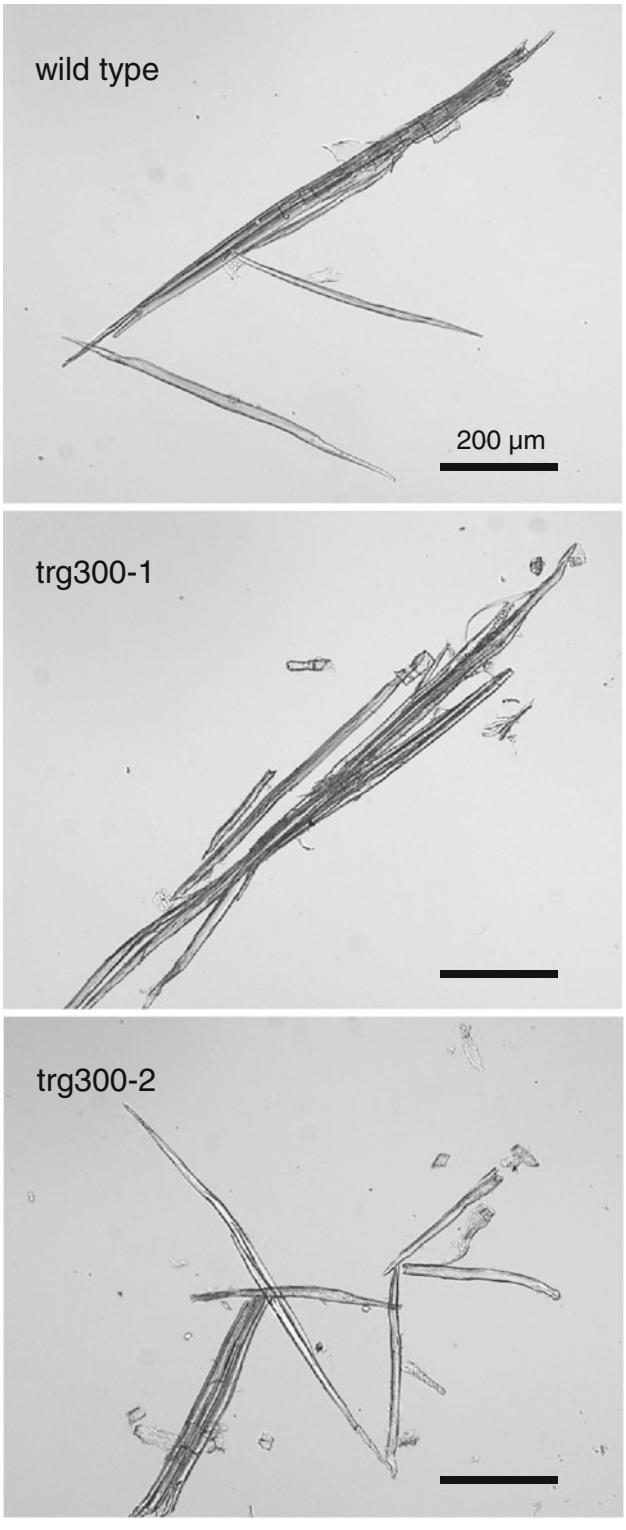

Fig. 1. Optical microscopic images of the holocellulose samples prepared from wild-type and transgenic (trg300-1 and trg300-2) poplars

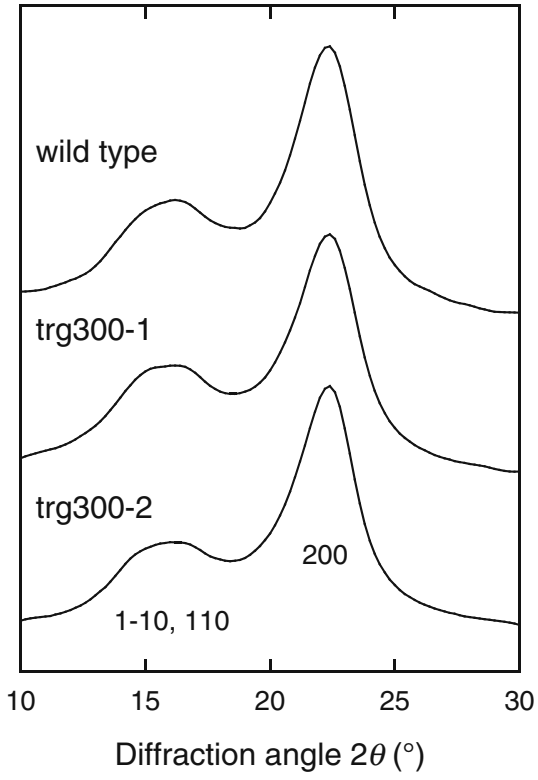

Fig. 2. X-ray diffraction patterns of the holocellulose samples prepared from the wild-type and transgenic (trg300-1 and trg300-2) poplars. *Numbers* indicate crystal planes

Table 1. Crystal widths and crystallinity indices of cellulose I in holocelluloses of wild-type and transgenic poplars calculated from the X-ray diffraction patterns shown in Fig. 2

Plant	Crystal width of (2 0 0) plane (nm)	Crystallinity index
Wild type	3.0	0.31
trg300-1	3.2	0.32
trg300-2	3.5	0.33

Table 2. Sugar compositions (%) of alkali-soluble polysaccharides (hemicelluloses) in holocelluloses of wild-type and transgenic poplars

Carbohydrate	Wild type	trg300-1	trg300-2
Cellulose	76.9	78.9	78.6
Hemicelluloses	23.1	21.1	21.4
Rhamnose	0.1	0.11	0.11
Fucose	0.03	n.d.	n.d.
Arabinose	0.38	0.31	0.32
Xylose	19.45	19.01	19.30
Mannose	1.36	0.72	0.73
Galactose	0.05	n.d.	n.d.
Glucose	1.74	0.95	0.96

n.d., not detected

for the wild type, trg300-1, and trg300-2 poplars, respectively (Table 1).

Table 2 shows the cellulose/hemicellulose ratios of the holocelluloses and the corresponding sugar compositions in the hemicellulose fractions. Based on acid hydrolysis, the hemicellulose in the transgenic plants contained decreased amounts of fucose, xylose, mannose, galactose, and glucose, all of which could be derived from the constitutive degradation of xyloglucan.[1] Among these, the decrease in mannose was probably due to a decrease in glucomannan content.

The cellulose contents were higher in the transgenic plants than in the wild type, although the differences were only 2% or less. Thus, the larger cellulose I crystal widths determined from X-ray diffraction patterns of the two holocelluloses of transgenic poplars were not explainable by the increased cellulose contents alone. Moreover, it is difficult to come to any conclusions about the differences in cellulose I crystal widths in the holocellulose samples from the X-ray diffraction data alone, because the crystallinity indices obtained were low.

Microfibrils prepared by TEMPO-mediated oxidation

In the next step, TEMPO-mediated oxidation was applied to the three holocellulose samples to individualize cellulose microfibrils by mild mechanical disintegration in water and to observe each fibril by TEM. Figure 3 shows TEM images of the microfibrils separated using this procedure. The cellulose microfibrils of the wild-type and trg300-1 poplars were well individualized in water (Figs. 3a and 3c), although some parts of the trg300-2 microfibrils were not completely separated and remained as bundles (Fig. 3e). The separated microfibrils had lengths ranging from 0.5 to 2 μm, irrespective of the type of holocellulose sample. Higher-magnification images are shown in Figs. 3b, 3d, and 3f. The microfibrils of transgenic poplars have apparently thicker widths than those of the wild type. The microfibril widths measured from the TEM images were 4.9 ± 0.6, 6.1 ± 0.7, and 6.0 ± 0.6 nm for the wild-type, trg300-1, and trg300-2 poplars, respectively. The *P* values of microfibril width when comparing the wild-type and trg300-1 poplars, the wild-type and trg300-2 poplars, and the trg300-1 and trg300-2 poplars were 5.7×10^{-7}, 6.7×10^{-7}, 0.60, respectively. Thus, it can be concluded at the 1% significance level that the cellulose microfibril widths of the transgenic poplars were larger than those of the wild-type poplar, whereas no significant difference in cellulose microfibril width was observed between the two

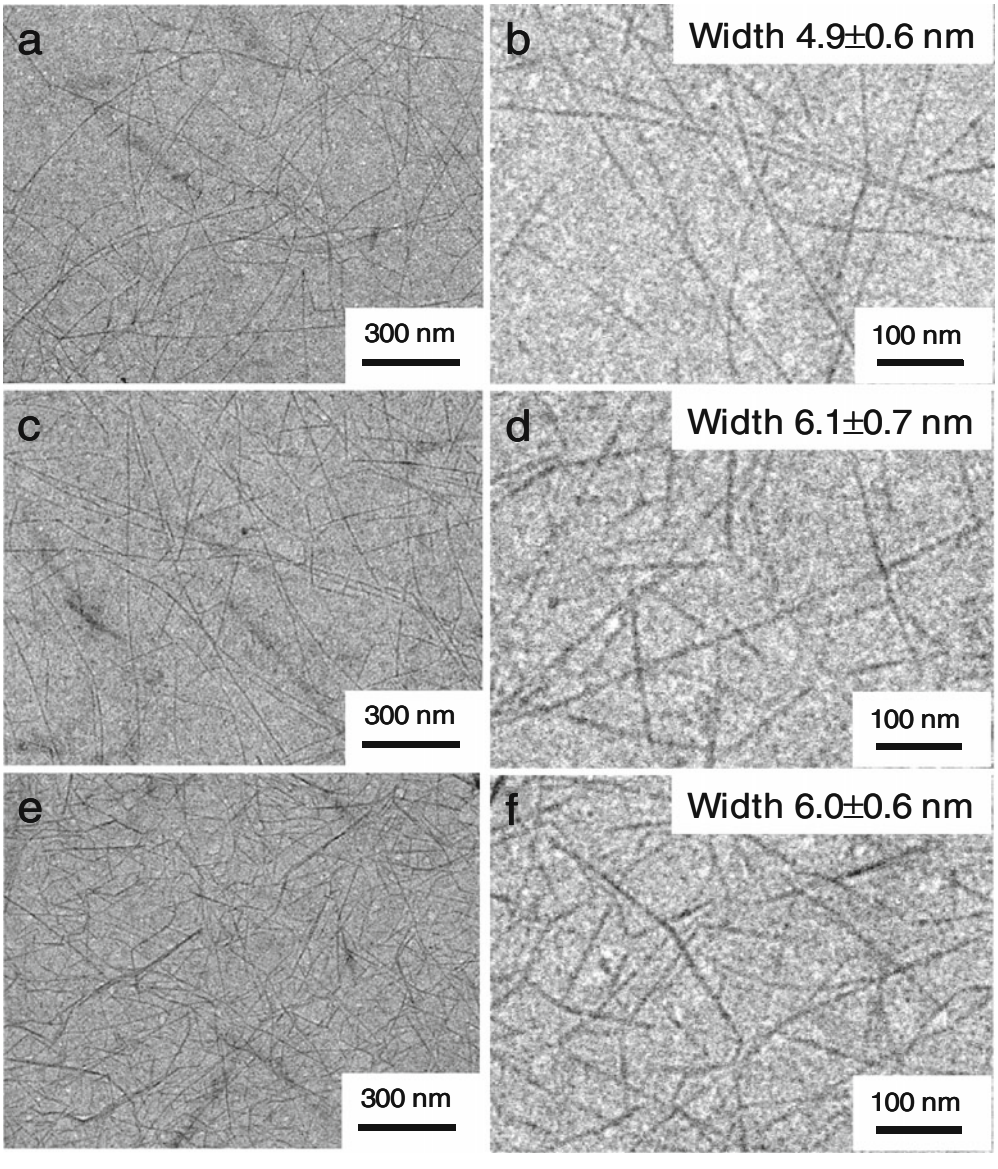

Fig. 3. Transmission electron microscopic images at two different magnifications of cellulose microfibrils prepared by the 2,2,6,6-tetramethylpiperidine-1-oxyl radical-oxidation method: wild type (**a**,**b**), trg300-1 (**c**,**d**) and trg300-2 (**e**,**f**)

transgenic poplars. There was no clear difference in the *P* values between the homo- and heteroscedasticities in all cases. Thus, cellulose microfibril width is enlarged in the fibers of the transgenic poplars as a result of the prevention of xyloglucan deposition.

Enlargement mechanism of cellulose microfibril width for transgenic poplars

The enlargement of cellulose microfibril widths for the transgenic poplars was, therefore, supported by both the X-ray diffraction and TEM methods. The data obtained here are in agreement with other findings[1,8,22] showing that the transgenic trees in which xyloglucan deposition was prevented had higher crystallinity values than the wild type did. However, there were somewhat large differences in absolute values between the cellulose microfibril widths measured from TEM images and the cellulose I crystal widths determined from X-ray diffraction patterns; the former values were always larger than those of the latter. Because some scattering effects are inevitable in TEM observations, the microfibril widths determined from TEM images might be somewhat overestimated. Moreover, because the increased cellulose content of the transgenic poplars was only 2% (Table 2), more than 20% increases from 4.9 to 6.0–6.1 nm in cellulose microfibril widths (Fig. 3) cannot be explained by the increased cellulose contents alone.

It is not plausible that the number of cellulose chains consisting of one elementary fibril formed from one rosette terminal complex increases for the transgenic poplars. Instead, even though the same number of cellulose chains is formed from one rosette terminal complex, some disordered regions present on each cellulose microfibril surface might be turned to more highly ordered structures in the transgenic poplars by a decrease in the amount of xyloglucan bound to the fibril surface. However, this hypothesis is speculative at present, and further studies to characterize the detailed structures of cellulose microfibril surfaces using atomic force microscopy and others are needed.

Acknowledgments This work was supported by JSPS Kakenhi (No. 100073500003). This article is also an outcome of the JSPS Global COE Program (E-04): In Search of Sustainable Humanosphere in Asia and Africa.

References

1. Park YW, Baba K, Furuta Y, Iida I, Sameshima K, Arai M, Hayashi T (2004) Enhancement of growth and cellulose accumulation by overexpression of xyloglucanase in poplar. FEBS Lett 564: 183–187
2. Taniguchi T, Omiya Y, Kurita M, Tsubomura M, Kondo T, Park YW, Baba K, Hayashi T (2008) Biosafety assessment of transgenic poplars overexpressing xyloglucanase (AaXEG2) prior to field trials. J Wood Sci 54:408–413
3. Nishikubo N, Awano T, Banasiak A, Bourquin V, Ibatullin F, Funada R, Brummer H, Teeri TT, Hayashi T, Sundberg B, Mellerowicz EJ (2007) Xyloglucan endo-transglycosylase (XET) functions in gelatinous layers of tension wood fibers in poplar – a glimpse into the mechanism of the balancing act of trees. Plant Cell Physiol 48:843–855
4. Baba K, Park YW, Kaku T, Kaida R, Takeuchi M, Yoshida M, Hosoo Y, Ojio Y, Okuyama T, Taniguchi T, Ohmiya Y, Kondo T, Shani Z, Shoseyov O, Awano T, Serada S, Norioka N, Norioka S, Hayashi T (2009) Xyloglucan for generating tensile stress to bend tree stem. Mol Plant 2:893–903
5. Park YW, Tominaga R, Sugiyama J, Furuta Y, Tanimoto E, Samejima M, Sakai F, Hayashi T (2003) Enhancement of growth by expression of poplar cellulase in *Arabidopsis thaliana*. Plant J 33:1099–1106
6. Shani Z, Dekel M, Tsabary G, Goren R, Shoseyov O (2004) Growth enhancement of transgenic poplar plants by overexpression of *Arabidopsis thaliana* endo-1,4-β-glucanase (*cel*1). Mol Breed 14:321–330
7. Hartati, S, Sudarmonowati, E, Park, YW, Kaku, T, Kaida, R, Baba, K, Hayashi, T (2008) Overexpression of poplar cellulase accelerates growth and disturbs the closing movements of leaves in sengon. Plant Physiol 147:552–561
8. Kaida, R, Kaku, T, Baba, K, Oyadomari, M, Watanabe, T, Nishida, K, Kanaya, T, Shani, Z, Shoseyov, O, Hayashi, T (2009) Loosening xyloglucan accelerates the enzymatic degradation of cellulose in wood. Mol Plant 2:904–909
9. Heyn AN (1969) Elementary fibril supermolecular structure of cellulose in soft wood fiber. J Ultrastruc Res 26:52–68
10. Fengel D (1978) Fibrillar structure of cellulose from wood. Holzforschung 32:37–44
11. Jakob HF, Fengel D, Tschegg SE, Fretzl P (1995) The elementary cellulose fibril in *Picea abies*: Comparison of transmission electron microscopy, small-angle X-ray scattering and wide-angle X-ray scattering results. Macromolecules 28:8782–8787
12. Saito T, Nishiyama Y, Putax JL, Vignon M, Isogai A (2006) Homogeneous suspensions of individualized microfibrils from TEMPO-catalyzed oxidation of native cellulose. Biomacromolecules 7: 1687–1691
13. Saito T, Kimura S, Nishiyama Y, Isogai A (2007) Cellulose nanofibers prepared by TEMPO-mediated oxidation of native cellulose. Biomacromolecules 8:2485–2491
14. Saito T, Isogai A (2004) TEMPO-mediated oxidation of native cellulose. The effect of oxidation conditions on chemical and crystal structures of the water-insoluble fractions. Biomacromolecules 5:1983–1989
15. Wise LE, Murphy M, Daddieco AA (1946) Chlorite holocellulose, its fractionation and bearing on summative wood analysis and on studies on the hemicelluloses. Tech Assoc Pap 29:210–218
16. Dubois M, Gilles KA, Hamilton JK, Rebers PA, Smith F (1956) Colorimetric method for determination of sugars and related substances. Anal Chem 28:350–356
17. Hayashi T (1989) Measuring β-glucan deposition in plant cell walls. In: Linskens HF, Jackson JF (eds) Modern methods of plant analysis: plant fibers. Springer-Verlag, Berlin, pp 138–160
18. Okita Y, Saito T, Isogai A (2010) Entire surface oxidation of various cellulose microfibrils by TEMPO-mediated oxidation. Biomacromolecules 11:1696–1700
19. Alexander LE (1979) X-ray diffraction methods in polymer science. Kreiger, New York, p 423
20. Wada M, Heux L, Sugiyama J (2004) Polymorphism of cellulose I family: Reinvestigation of cellulose IV. Biomacromolecules 5:1385–1391
21. Sugiyama J, Vuong R, Chanzy H (1991) Electron diffraction study on the two crystalline phases occurring in native cellulose from an algal cell wall. Macromolecules 24:4168–4175
22. Kaida R, Kaku T, Baba K, Hartati S, Sudarmonowati E, Hayashi T (2009) Enhancement of saccharification by overexpression of poplar cellulase in sengon. J Wood Sci 55:435–440